

PS07: การศึกษา Sawtooth Oscillations กับการให้พลังงานแบบ ECRH ใน พลาสมาของเครื่องโทคาแมค HL-2A ด้วยแบบจำลอง 1.5D BALDUR

*จิราภรณ์ พรหมพิงค์¹ ธวัชชัย อ่อนจันทร์² นพพร พูลยรัตน์¹ และรพชน พิชา³

¹ภาควิชาฟิสิกส์ คณะวิทยาศาสตร์และเทคโนโลยี มหาวิทยาลัยธรรมศาสตร์

ต.คลองหนึ่ง อ.คลองหลวง จ.ปทุมธานี 12120

โทรศัพท์ 0 2986 9009 โทรสาร 0 2986 9112-3 E-Mail: ame026@gmail.com

²หน่วยวิจัยพลาสมา และ ฟิวชัน สถาบันเทคโนโลยีนานาชาติสิรินธร มหาวิทยาลัยธรรมศาสตร์ ต.คลองหนึ่ง อ.

คลองหลวง จ.ปทุมธานี 12120

³สถาบันเทคโนโลยีนิวเคลียร์แห่งชาติ (องค์การมหาชน) เขตจตุจักร กรุงเทพฯ 10900

บทคัดย่อ

การสั่นแบบซอว์ทูธ (sawtooth oscillations) เป็นความไม่เสถียรของพลาสมาในเครื่องโทคาแมครูปแบบหนึ่ง และเป็นปัญหาที่สำคัญของการศึกษาพลาสมาในเครื่องโทคาแมคอย่างหนึ่ง เนื่องจาก การเกิดลุ่มแบบซอว์ทูธ (sawtooth crash) มีผลทำให้อุณหภูมิและความหนาแน่นที่ตรงกลางของพลาสมาลดลง อันจะทำให้ประสิทธิภาพของพลังงานนิวเคลียร์ที่ได้ลดลงตามไปด้วย ในงานวิจัยนี้จะทำการศึกษาปรากฏการณ์การเกิดการสั่นแบบซอว์ทูธในช่วงการให้พลังงานแบบ ECRH ในเครื่องโทคาแมค HL-2A โดยใช้แบบจำลองทางคณิตศาสตร์แบบรวมที่มีชื่อว่า 1.5D BALDUR ในแบบจำลองนี้ พลาสมาในส่วนกลางของเครื่องโทคาแมคสามารถอธิบายได้จากผลรวมของการแพร่ (transport) จากสองส่วนคือ anomalous transport และ neoclassical transport สำหรับงานวิจัยนี้ เราได้ใช้แบบจำลอง Multimode (MMM95) สำหรับ anomalous transport และใช้ NCLASS สำหรับ neoclassical transport ทั้งนี้จะใช้แบบจำลองในการทำนายการเกิด sawtooth oscillation 3 แบบ คือ Rogers-Zakharov model, Park-Monticello model และ Porcelli model

คำสำคัญ: การสั่นแบบซอว์ทูธ ความไม่เสถียรของพลาสมา โทคาแมค พลาสมา

The Study of Sawtooth Oscillation during ECRH of HL-2A-like Plasma using 1.5D BALDUR Code

*J. Promping¹, T. Onjun² N. Poolyarat¹ and R. Picha³

¹Department of Physics, Faculty of science and Technology

Thammasat University, Klong Luang, Phatum-Thani, Thailand, 12120

Phone: 0 2986 9009, 0 29869101, Fax: 0 2986 9112-3, E-Mail: ame026@gmail.com

²Plasma and Fusion Research Unit, Sirindhorn International Institute of Technology

Thammasat University, Klong Luang, Phatum-Thani, Thailand, 12120

³Thailand Institute of Nuclear Technology, Bangkok, Thailand, 10900

Abstract

One of the current issues in tokamak plasma is sawtooth oscillation, because each sawtooth crash results in a significant decrease of central temperature and density. Consequently, the nuclear fusion power will drop. This has a significant impact on the performance of future nuclear fusion power plants. In this work, behaviors of sawtooth oscillations during an electron-cyclotron resonant heating (ECRH) in HL-2A tokamak experiment are studied. The simulation of plasma in HL-2A tokamak is carried out using the 1.5D BALDUR integrated predictive modeling code, where the plasma core can be described by the combination of anomalous and neoclassical transport. For the anomalous transport, we use Multimode (MMM95) model, while for the neoclassical transport, we use the NCLASS module. In each simulation, a sawtooth crash is predicted by either Rogers-Zakharov sawtooth triggering model, Park-Monticello sawtooth triggering model, or Porcelli sawtooth triggering model.

Keywords: sawtooth crash sawtooth triggering tokamak plasma

1. Introduction

A BALDUR integrated predictive modeling code¹ has been developed to simulate the time evolution of the tokamak plasma current, temperature, and density profiles. This code computes the sources, sinks, and transport of thermal energy and particle fluxes, as well as the equilibrium shape of the plasma and the effects of large-scale instabilities. The BALDUR simulation with predictive core transport models, such as Mixed Bohm/ gyro Bohm (Mixed B/gB) or Multimode (MMM95), has successfully reproduced many experiments in a wide range of plasma scenarios from various large tokamaks; such as JET^{2, 3}, DIII-D^{2, 3}, Tore Supra⁴ and Alcator C-MOD⁵. These simulations yield better understanding of the physical processes and the inter-relationships among these physical processes that occur in tokamak plasma experiments. Finally, it results in advance of nuclear fusion.

In this work, self-consistent simulations are carried out using BALDUR code. The simulations are carried out with plasma parameters similar to those for an HL-2A discharge number 4343. This discharge includes an Electron Cyclotron Resonance Heating (ECRH), which aims to observe the transport behavior and sawtooth oscillation. The BALDUR simulations provide an insight understanding of plasma behavior in the HL-2A experiment⁶.

2. Modeling Code

2.1 BALDUR code

The BALDUR code is an integrated predictive modeling code developed to compute the time evolution of plasma profiles including electron and ion temperatures, deuterium, tritium, helium and impurity densities, magnetic q , neutrals, and fast ions. These time-evolving profiles are computed by combining the effects of many physical processes self-consistently, including the effects of transport, plasma heating, particle influx, boundary conditions, the plasma equilibrium shape, and sawtooth oscillations. Fusion heating and helium ash accumulation are also computed self-consistently. The BALDUR simulations have been intensively compared against various plasma experiments, which yield an overall agreement with 10% relative RMS deviation^{2, 3}. In BALDUR code, fusion heating power is determined by the nuclear reaction rates and a Fokker Planck package to compute the slowing down spectrum of fast alpha particles on each flux surface in the plasma¹. The fusion heating component of the BALDUR code also computes the rate of the production of thermal helium ions and the rate of the depletion of deuterium and tritium ions within the plasma core. In this work, the BALDUR code together with an anomalous transport model is used to carry out simulations. The brief details of a choice of an anomalous transport models are described below.

2.2 Multimode model (MMM95)

MMM95 model⁷ is a linear combination of theory-based transport models which consists of the Weiland model for the ion temperature gradient (ITG) and trapped electron modes (TEM), the Guzdar–Drake model for drift-resistive ballooning modes (RB), as well as a smaller contribution from kinetic ballooning modes (KB). For large tokamak simulations, the drift wave Weiland model for drift modes such usually provides the largest contribution to the MMM95 transport model in most of the plasma core. The Weiland model is derived by linearizing the fluid equations, with magnetic drifts for each plasma species. Eigen values and eigenvectors computed from these fluid equations are then used to compute a quasilinear approximation for the thermal and particle transport fluxes. The Weiland model includes many different physical phenomena such as effects of trapped electrons, $T_i \neq T_e$, impurities, fast ions, and finite β . The resistive ballooning model in MMM95 transport model is based on the 1993 $E \times B$ drift-resistive ballooning mode model by Guzdar–Drake, in which the transport is proportional to the pressure gradient and collision. The

contribution from the resistive ballooning model usually dominates the transport near the plasma edge. Finally, the kinetic ballooning model is a semi-empirical model, which usually provides a small contribution to the total diffusivity throughout the plasma, except near the magnetic axis. All the anomalous transport contributions to the MMM95 transport model are multiplied by K^{-4} , since the models were originally derived for circular plasmas.

2.3 Sawtooth Oscillations

Sawtooth oscillations⁸ are periodic relaxation oscillations of the plasma temperature, density and other plasma parameters in the central region of a tokamak, which develop when the magnetic winding index on axis, q_0 drops below unity. A slow rise (the sawtooth ramp), determined by transport and heating, is followed by a rapid drop (the sawtooth crash), triggered by the instability of an internal kink mode with toroidal $n = 1$ and dominant poloidal $m = 1$ mode number (in short, an $m = 1$ mode). The temperature and density profiles become flat after each sawtooth crash, up to the *mixing radius*, r_{mix} which is somewhat larger than the $q = 1$ radius of the pre-crash q profile. The current density also changes during this sequence, although experimental evidence indicates that complete flattening of the q profile does not always occur.

2.3.1 Park-Monticello Sawtooth model

In Park-Monticello sawtooth model¹⁰, the sawtooth period is predicted to be

$$\tau_{Park-Monticello} = C_0 \times 0.009 \times \frac{R^2 T_{e,0}^{1.5}}{z_{eff}} \quad (7)$$

where C_0 is a constant usually taken to be 1.

2.3.2 Rogers-Zakharov Sawtooth model

The Rogers-Zakharov sawtooth model¹¹ is based on one fluid MHD instability of the $m = 1$ mode at $r = r_{q=1}$. First, we consider whether $j'' = (r_1) > 0$ or $\Lambda_H < 0$, where j'' is current and

$$\Lambda_H = \frac{r_1^2}{R^2} \left(\frac{13}{64} b - \frac{c}{4(1-c)} \beta_p^2 \right) \quad (8)$$

This mode is unstable and we set $s_0 = 0$, where s_0 is a lower bound shear. Otherwise, the lower bound shear is given by

$$s_0 = \left(\frac{\pi \sqrt{6} \Lambda_H \sqrt{-j_1'' r_1^2}}{4} \right)^{0.4} \quad (9)$$

Next, we consider the finite Larmor radius stabilized ideal mode. This mode is unstable if the shear is less than

$$s_H = -\Lambda_H \frac{\omega_{pi} r_1}{c} \left| \frac{B^2}{4p'_i R} \right| \quad (10)$$

where the ion plasma frequency is given by

$$\omega_{pi} = \sqrt{4\pi \sum_{ions} n_i Z_i^2 e^2 / m_i} \quad (11)$$

Finally, consider the $m=1$ tearing mode stabilized by finite Larmor radius effects (collisionless tearing modes). The critical shear is

$$s_{CD} = \sqrt{\frac{m_i}{m_e}} \left| \frac{2\pi p'_i R}{B^2} \right| \frac{C_{sawtooth}}{1 + 0.4 \sqrt{\beta m_i / m_e}} \quad (12)$$

Where p'_i is the gradient of the thermal ion pressure at r_1 , β is the total beta including fast ions, and m_i is the densityweighted ion mass. The default value of $C_{sawtooth}$ should be 1.0. Now compare the shear at the $q=1$ surface with the critical shear. The condition for a sawtooth crash is

$$s_H > shear > s_0 + s_{CD} \quad (13)$$

2.3.3 Porcelli Sawtooth model

In Porcelli sawtooth model¹², the sawtooth crashes are triggered when one of the following conditions is met:

$$-\delta \hat{W}_{core} > c_h \omega_{DH} \tau_A \quad (14)$$

$$-\delta \hat{W} > 0.5 \omega_{*i} \tau_A \quad (15)$$

$$-c_\rho \hat{\rho} < -\delta \hat{W} < 0.5 \omega_{*i} \tau_A \text{ and } \omega_{*i} < c_* \gamma_\rho \quad (16)$$

where c_ρ and c_* are constants and

$$\delta \hat{W} \equiv \text{core functional energy} \propto \varepsilon_1^2 \beta_{p1}^2$$

$$\gamma_\rho \approx 1.1 \frac{6/7}{s_1} \hat{\rho}^{4/7} / (\tau_A s^{1/7}) \quad (17)$$

3. Experimental Observations

Recent HL-2A experiments with ECRH heating were reported by S ZhongBing et.al¹⁴. In those experiment, HL-2A was operated with the ECRH heating power of 450 kW with a duration of $t_{ECRH} = 700 \sim 1030$ ms with on-axis or off-axis heating scheme. In the case of on-axis heating scheme, the time evolution of electron temperature profiles are found to be peaked, while in case of off-axis the electron profiles are found to be flat.

In that paper, the time evolution of both the sawtooth period and electron density during ECRH experiment are also presented. It is observed that just after launching the ECRF power into

the plasma, the sawtooth becomes a dual or compound form, and about 20 ms later the sawtooth period decreases as the core plasma density decreases, while the density in the diverter increases. It indicates that the dependence of the sawtooth period upon the plasma density is stronger than that upon the heating power or plasma temperature. This may be evidence that particles in plasma are ejected from the sawtooth region, leading to an outward propagation of the plasma density.

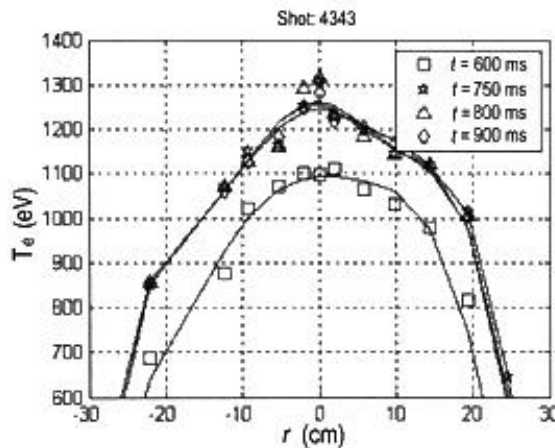


Fig 1 Time evolution of electron temperature profiles at on-axis off-axis ECRH¹⁴

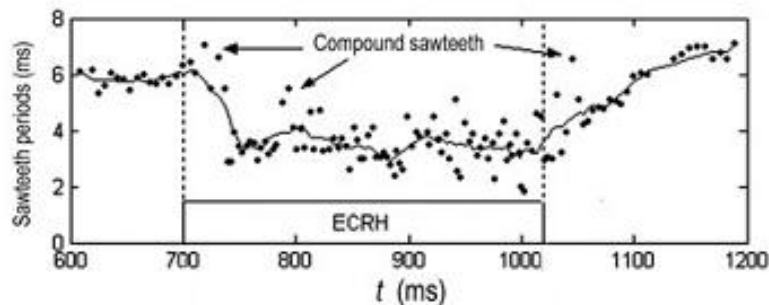


Fig 2 Sawteeth periods and electron density versus time during ECRH experiment¹⁴

4. Results and Discussions

The BALDUR integrated predictive modeling code is used to carry out the plasma of the HL-2A experiment discharge number 4343 (with ECRH heating). The parameters used in the simulation are shown in Table 1. In this work, the plasma density and plasma current are ramped up to the target values within 0.2 s. It is found that the plasma reaches the *H*-mode phase at the time of 0.7 s, right after an ECRH heating of 0.45 MW is turned on. Note that a transition for *L*-mode to *H*-

mode occurs when the heating power exceeds the power threshold. In these simulations, the sawtooth oscillation is considered during the time of 0.1 s to 1.5 s. For each simulation, an anomalous transport is calculated using the MMM95 transport model, while a neoclassical transport is computed using the NCLASS module. The boundary conditions are provided at the top of the pedestal by the pedestal model¹³ once the plasma entering the *H*-mode phase. It is assumed that the electron and ion pedestal temperatures are of the same values. In most simulations, the auxiliary heating power of 0.45 MW, which is assumed to fully heat the electron, is used. The effect of sawtooth oscillation is also included, where Rogers-Zakharov sawtooth triggering model, Park-Monticello sawtooth triggering model and Porcelli sawtooth triggering model is used to determine a sawtooth crash and a modified Kadomtsev magnetic reconnection model is used to describe the effects of sawtooth crash.

Table 1 Plasma parameters for HL-2A discharge 4343

Parameter	Physical Description	Values
R (m)	Major radius	1.65
a (m)	Minor radius	0.40
I_p (MA)	Plasma current	0.25
B_T (T)	Toroidal field	2.43
κ_{95}	Elongation	1.30
δ_{95}	Triangularity	0.30
Z_{eff}	Effective charge	1.50
P_{aux} (MW)	Auxiliary power	0.45

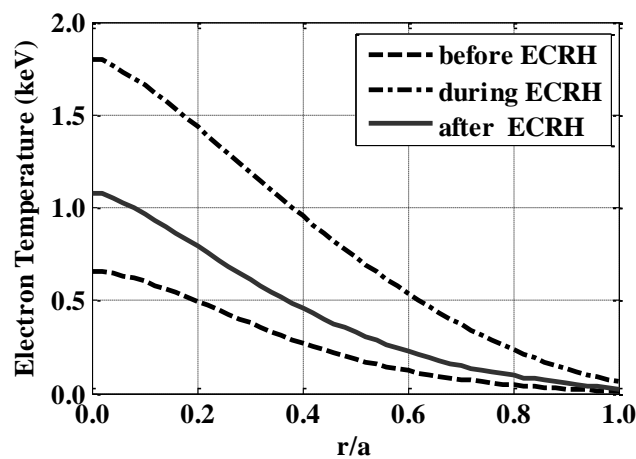


Fig 3 Profiles for electron temperature are shown as a function of normalize minor radius at a time before, during and after heating phase. This simulation of a sawtooth crash is predicted by using Park-Monticello sawtooth triggering model.

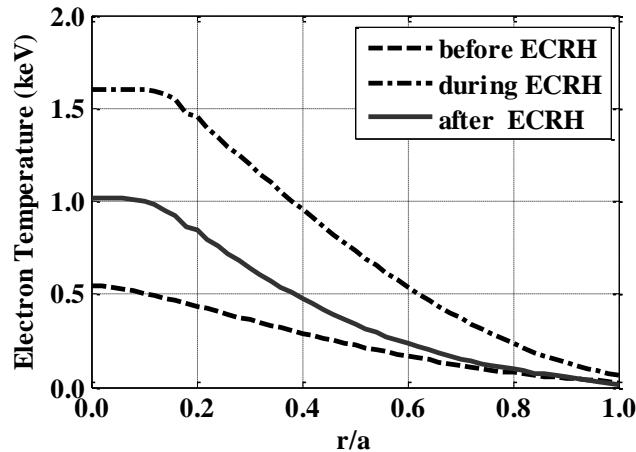


Fig 4 Profiles for electron temperature are shown as a function of normalize minor radius at a time before, during, and after heating phase. This simulation of a sawtooth crash is predicted by using Rogers-Zakharov sawtooth triggering model.

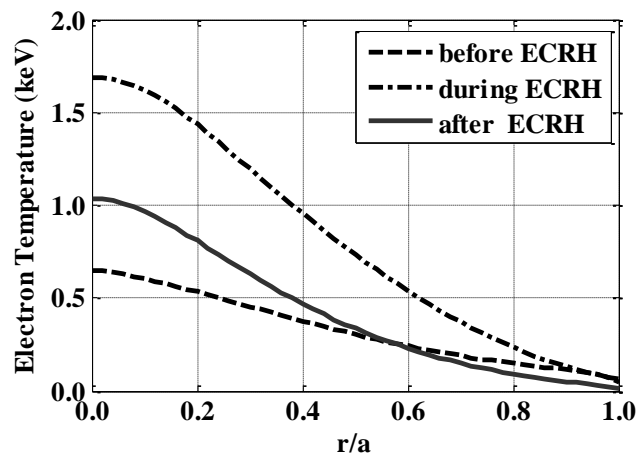


Fig 5 Profiles for electron temperature are shown as a function of normalize minor radius at a time before, during and after heating phase. This simulation of a sawtooth crash is predicted by using Porcelli sawtooth triggering model.

Figures 3, 4 and 5 show the electron temperature as a function of the normalized minor radius at the time before sawtooth crash using Park-Monticello, Rogers-Zakharov, and Porcelli triggering models, respectively. It can be seen that the electron temperature profiles are peak

profiles.. The central and average values from each simulation are summarized in Table 2. Note that these values are at the time before sawtooth crash. When an auxiliary heating is applied, the temperature near the center increases. After the heating is turned off, the temperature drops. This result is similar to that observed experimentally in Ref.[14]. It was found in the experiment that the central electron temperature increases from 1.10 keV to 1.25 keV when the heating is applied. The values obtained from the BALDUR simulations are in the range of experimental observation.

Table 2 The averaged central electron temperatures obtained from different models and experiment

Sawtooth triggering model	$T_{e,0}$ (eV)		
	Before heating	During heating	After heating
Experimental	1100	1250	-
Park-Monticello	659.4	1795.4	1095.3
Rogers-Zakharov	544.4	1603.7	1015.3
Porcelli	646.5	1688.7	1038.5

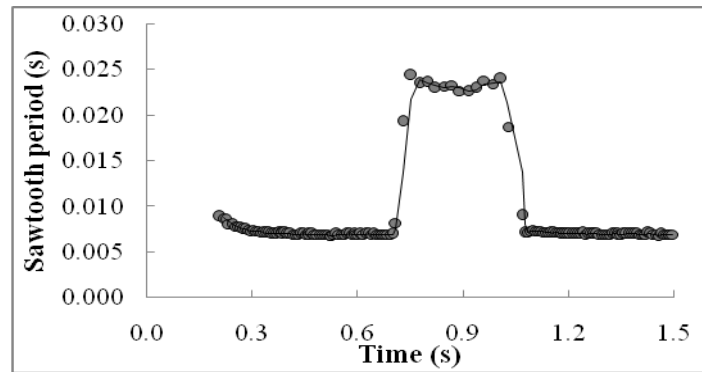


Fig 6 The sawtooth period are plotted as a function of time. The ECRH is turned on during $t=700-1030$ ms. This simulation of a sawtooth crash is predicted by using Park-Monticello sawtooth triggering model.

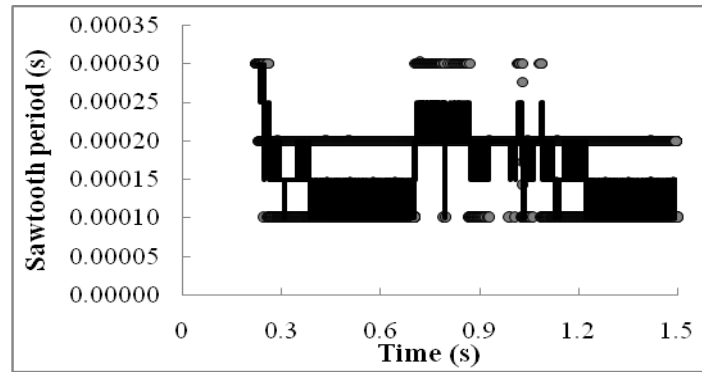


Fig 7 The sawtooth period are plotted as a function of time. The ECRH is turned on during $t=700-1030$ ms. This simulation of a sawtooth crash is predicted by using Rogers-Zakharov sawtooth triggering model.

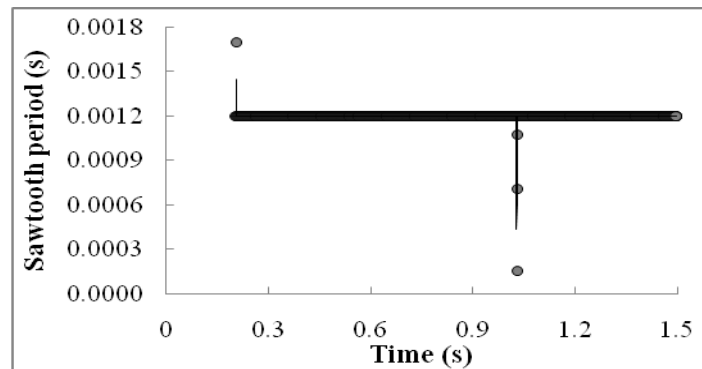


Fig 8 The sawtooth period are plotted as a function of time. The ECRH is turned on during $t=700-1030$ ms. This simulation of a sawtooth crash is predicted by using Porcelli sawtooth triggering model.

Figures 6 and 7 show the sawtooth period as a function of time from a simulation using the MMM95 transport models, these simulations of a sawtooth crash use Park-Monticello and Rogers-Zakharov sawtooth triggering models, respectively. It can be seen that the sawtooth period decreased during the heating phase in the simulations using and MMM95 model. This result is opposite to that observed in experiment. In Figure 8, sawtooth periods are plotted as a function of time from a simulation using the MMM95 transport models with the Porcelli sawtooth triggering model. It can be seen that the sawtooth period remains unchanged during the heating phase. The values of sawtooth period from each simulation are summarized in Table 3. It was found in the experiment that the sawtooth period decreases from 6 ms to 3 ms when the heating is applied. The values obtained from the BALDUR simulations are not in the range of experimental observation.

Table 3 The average sawtooth period from each model are summarized in the table

Sawtooth triggering model	Sawtooth period (s)		
	Before heating	During heating	After heating
Experimental	0.00600	0.00300	0.00600
Park-Monticello	0.00700	0.02280	0.00700
Rogers-Zakharov	0.00015	0.00021	0.00015
Porcelli	0.00120	0.00120	0.00120

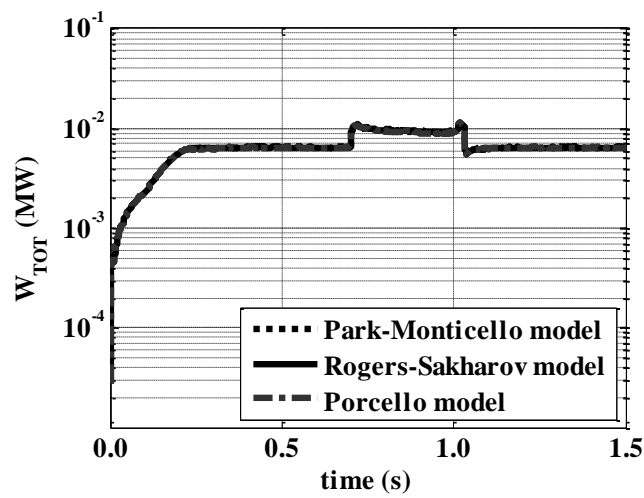


Fig 9 The total stored energy are plotted as a function of time. The dotted line is based on Park-Monticello model, the dashed line is based on Rogers-Sakharov model and the dashed-dotted line is based on Porcelli model. The ECRH is turned on during $t=700-1030$ ms.

Figure 9 shows the total stored energy as a function of time. All three sawtooth triggering models yield the same result. Furthermore, it can be seen that the total stored energy suddenly increased during the heating phase about 20 times in the simulations. Due to this constraint, we run the simulation to understand the consequence in the temperature profile results.

5. Conclusion

The simulations for HL-2A-like plasma are carried out using the 1.5D BALDUR integrated predictive modeling code using the MMM95 as a core transport model together with either using the Park-Monticello model, the Rogers-Zakharov model, or the Porcelli model as the sawtooth

triggering model. The simulation results from all sawtooth triggering models show that electron temperature profile is increased during the ECRH, which is in agreement with the experimental observations. As for the sawtooth period during the ECRH, both Park-Monticello model and Rogers-Zakharov model predict the increased period compared to the value before the ECRH, while Porcelli model predicted the period to remain the same. These results are in contradiction with the experimental observation of HL-2A tokamak. More attention will be required both on the experimental observation from other tokamaks and on the sawtooth triggering models.

6. Acknowledgments

The research is supported by the Ministry of Science and Technology "Researchers and Developers in Science and Technology Support Project" and Thammasat University Research Fund 2551.

7. References

1. Singer, C. E, et al., 1988. A one-dimensional plasma transport code, *Comput. Phys. Common*, **49**, pp.275-398.
2. Hannun, D. Bateman, G. Kinsey, J. et al., 2001. Comparison of high-mode predictive simulations using Mixed Bohm/gyro-Bohm and Multi-Mode (MMM95) transport models, *Physics of Plasmas*, **8**, pp.964-974.
3. Onjun, T. Bateman, G. Kritz, A.H. et al. Comparison of low confinement mode transport simulations using the mixed Bohm/gyro-Bohm and the Multi-Mode-95 transport model, *Physics of Plasmas*, **8**, pp.975-985.
4. Voitsekhovitch, I. Bateman, G. Kritz, A.H. et al., 2002. Predictive simulations of radio frequency heated plasmas of Tore Supra using the Multi-Mode model, *Physics of Plasmas*, **9**, pp.4241-4251.
5. Pankin, A. Bateman, G. Kritz, A.H. et al. Alcator C-mod predictive modeling, *Physics of Plasmas*, **8**, pp.4403-4413.
6. Yong, L. Xuantong, D. Qingwei, Y. et al., 2005. *Nuclear Fusion*, **45**, S239.

7. Bateman G, Kritz A.H, Kinsey J.E, et al., 1998. Predicting temperature and density profiles in tokamaks. *Physics of Plasmas*, **5**, 1793-1799.
8. Von Goeler S, Stodiek W and Sauthoff N., 1974. *Phys. Rev. Let*, **33**, 1201.
9. Bateman, G. Nguyen, C.N. Kritz. A.H. et al., 2006. Testing a model for triggering sawtooth oscillations in tokamaks, *Plasma Physics and Controlled Fusion*, **6**, **13**, 072505.
10. Park, W. Monticello, D., 1990. *Princeton plasma physics laboratory*, 2601.
11. Rogers, B. Zakharov, L., 1995. Nonlinear omega_{*}-stabilization of the m=1 mode in tokamaks, *Physics of Plasmas*, **5**, pp.3420-4328.
12. Porcilli, F. Boucher, D. Rosenbluth, MN, 1996. Model for the sawtooth period and amplitude, *Plasma Physics and Controlled Fusion*, **38**, pp.2163-2186.
13. Onjun, T. Bateman, G. Kritz, A.H. et al., 2002. Models for the pedestal temperature at the edge of H-mode tokamak plasmas, *Physics of Plasmas*, **9**, pp.5018.
14. ZhongBing, S. Xuantong, D. Jun, R. et al., 2007. Preliminary Results of Sawtooth Behaviour and Electron Heat Transport during ECRH Experiment on HL-2A, *Plasma Science and Technology*, **9**, 5.